10.24425/acs.2023.146428

Archives of Control Sciences
Volume 33(LXIX), 2023
No. 2, *pages 425–458*

Fractional order $PI^{\lambda}D^{\mu}A$ controller design based on Bode's ideal function

Khalfa BETTOU and Abdelfatah CHAREF

The fractional order proportional, integral, derivative and acceleration ($PI^{\lambda}D^{\mu}A$) controller is an extension of the classical PIDA controller with real rather than integer integration action order λ and differentiation action order μ. Because the orders λ and μ are real numbers, they will provide more flexibility in the feedback control design for a large range of control systems. The Bode's ideal transfer function is largely adopted function in fractional control systems because of its iso-damping property which is an essential robustness factor.

In this paper an analytical design technique of a fractional order $PI^{\lambda}D^{\mu}A$ controller is presented to achieve a desired closed loop system whose transfer function is the Bode's ideal function. In this design method, the values of the six parameters of the fractional order $PI^{\lambda}D^{\mu}A$ controllers are calculated using only the measured step response of the process to be controlled. Some simulation examples for different third order motor models are presented to illustrate the benefits, the effectiveness and the usefulness of the proposed fractional order $PI^{\lambda}D^{\mu}A$ controller tuning technique. The simulation results of the closed loop system obtained by the fractional order $PI^{\lambda}D^{\mu}A$ controller are compared to those obtained by the classical PIDA controller with different design methods found in the literature. The simulation results also show a significant improvement in the closed loop system performances and robustness using the proposed fractional order $PI^{\lambda}D^{\mu}A$ controller design.

Key words: Bode's ideal transfer function, fractional order control, classical PIDA controller, fractional order $PI^{\lambda}D^{\mu}A$ controller, robustness

1. Introduction

A non-intuitive and difficult task to control engineers is the design of an effective and economic controller. The most commonly used controllers in the process control industry are the proportional, integral and derivative (PID) controllers [1, 2]. Since Ziegler and Nichols have presented their PID controller

K. Bettou (corresponding author, e-mail: bettou_kh@yahoo.com) and A. Charef (e-mail: afcharef@yahoo.com) are with Laboratoire de Traitement du Signal, Département d'Electronique, Université des Frères Mentouri – constantine, Route Ain El-bey, Constantine 25011, Algeria.

Received 26.09.2022. Revised 25.04.2023.

parameters tuning method [3], a continuous research work is still underway towards system control quality improvement and performance enhancement. In many control applications, the processes are modeled as third order systems. The classical PID controllers become unsuitable for the control of these third order systems; hence a new controller structure becomes necessary for such systems [4].

In 1996, Jung and Dorf have introduced the proportional integral derivative accelerated (PIDA) controller which is more suitable for feedback control systems of higher order plants [5]. They have found that the feedback control system with the PIDA controller has delivered a faster and a smoother response than the feedback control system with the PID controller for third-order systems. The idea behind the PIDA controller design is to add an extra zero in classical PID controller. A New Analytical approach of PIDA design was proposed by Kitti's in [6], and extended to discrete system [7]. Some optimal designs of the PIDA controller were presented using several optimization algorithms [8–11].

The application of PIDA controller was successfully carried out for several applications, a servo motor driving, a load through a long shaft or transmission system in [12], an induction motor control in [13, 14], an automatic voltage regulator system in [15, 16], a power system in [17, 18], a Liquid-Level System in [19], a Cardiac Pacemaker in [20], and a Temperature Control of Electric Furnace System in [21].

In recent years, the emergence of new computational techniques for fractional calculus has made possible the transition from classical models and controllers to those described mathematically by differential equations of non integer order. Thus, fractional-order dynamic models and controllers have been introduced. The interest in fractional order control can be traced back to the late nineteenth century. The growing tendency towards using fractional order control has been fueled mainly by the fact that these controllers have additional tuning knobs that allow coherent adjustment of the dynamics of control systems [22, 23].

Different from the classical linear integer order PID controller, fractional order $PI^{\lambda}D^{\mu}$ controller is nonlinear naturally regarding the fractional order, which brings the main difficulties in system design and analysis.

Nowadays, various design methods have been proposed for fractional order $PI^{\lambda}D^{\mu}$ controller tuning. In [24], the basic ideas are based on already existing classical PID controllers and the minimum ISE criterion for setting the fractional integration action order and the fractional differentiation action order. The well–known Ziegler-Nichols tuning rule has been extended to fractional order $PI^{\lambda}D^{\mu}$ controller with S-shaped step response, but it only works well on some lag dominant process [25]. For a typical first order plus dead time model, some tuning rules are developed to minimize integrated absolute error (IAE) subject to a constraint on the maximum sensitivity [26]. To obtain good control performance, dominant pole placement for fractional order $PI^{\lambda}D^{\mu}$ controller is developed based on D-decomposition method [27]. In the last years, the internal model control

(IMC) tuning method is also introduced in the design of fractional order $PI^{\lambda}D^{\mu}$ controller [28, 29].

Bode shaping is an effective method for control system design in frequency domain. As a good open loop model, Bode's ideal transfer function is discussed in [30], which shows its stronger robustness against loop gain variation. To realize auto-tuning of fractional order $PI^{\lambda}D^{\mu}$ controller, online optimization technologies are employed to optimize the Bode's model and controller parameters [31]. In [32], a model-based analytical method is developed for fractional order $PI^{\lambda}D^{\mu}$ controller design via internal model control (IMC) principle and Bode's model.

Various papers have proposed different optimization tuning methods for fractional order $PI^{\lambda}D^{\mu}$ controller. In [33], a method based on solving a set of nonlinear equations is proposed. In [34], a tuning rule for fractional order $PI^{\lambda}D^{\mu}$ controller suitable for motion systems is given. In [35], Modified Grey Wolf Optimizer is adopted to design the fractional order $PI^{\lambda}D^{\mu}$ controller. Another class of fractional order $PI^{\lambda}D^{\mu}$ controller is proposed in [36], which ensures robustness to the closed-loop static gain variation of traditional CRONE templates [37].

A multi-objective extremal optimization algorithm is adopted to design fractional order $PI^{\lambda}D^{\mu}$ controller, [38, 39]. Besides, there are some effective fractional order $PI^{\lambda}D^{\mu}$ tuning settings summarized in [23].

Therefore, this article combines fractional calculus with classical PIDA controller [5, 40]. Fractional order $PI^{\lambda}D^{\mu}A$ controller is a generalization of classical PID controller considering fractional derivative and integral action and integer acceleration action. The fractional order $PI^{\lambda}D^{\mu}$ controller is proposed by Professor I. Podlubny [40], and is generally simply expressed as $PI^{\lambda}D^{\mu}$.

Compared with classical PIDA controller, fractional order $PI^{\lambda}D^{\mu}A$ controller adds two different parameters to be adjusted: integral order and differential order, which makes the setting range of the control parameters larger. Therefore, better robust control effect can be obtained.

At present, many studies have explored the characteristics of fractional order $PI^{\lambda}D^{\mu}A$ and compared its performance with classical PIDA controller in different environments [41–46].

In this paper, a new analytical method of designing the fractional order $PI^{\lambda}D^{\mu}A$ controller for classical feedback control systems is proposed. This method uses the step response of the process and requires no approximation of the process by any model. Inspired from a recent PID and fractional order $PI^{\lambda}D^{\mu}$ design techniques, the proposed method makes use of the Taylor–Maclaurin series development [47, 48]. The six parameters of the fractional order $PI^{\lambda}D^{\mu}A$ controller are tuned such that the closed loop system is equivalent to a desired fractional order model whose transfer function is Bode's ideal function, called in this context the fractional order relaxation or oscillatory system [49]. This type of fractional order system is widely used in the fractional order control domain

because it has the iso-damping property which is a very important robustness feature.

The basic ideas of the design method are presented and the formulae for the calculation of these tuning parameters are derived analytically. Illustrative examples were presented to test the effectiveness and the usefulness of the proposed fractional order $PI^{\lambda}D^{\mu}A$ controller design method. These results are concluded in conclusion.

2. Preliminaries

2.1. Brief introduction to fractional order calculus

A commonly used definition of fractional differo-integral is the Riemann-Liouville definition

$$ {}_aD_t^{\alpha} f(t) = \frac{1}{\Gamma(m-\alpha)} \left(\frac{d}{dt}\right)^m \int_a^t \frac{f(\tau)}{(t-\tau)^{1-(m-\alpha)}} \mathrm{d}\tau \,. \tag{1} $$

For $m-1 \prec \alpha \prec m$; where, $\Gamma(.)$ is the well-known Euler's gamma function. An alternative definition, based on the concept of fractional differentiation, is Grunwald-Letnikov definition given by

$$ {}_aD_t^{\alpha} f(t) = \lim_{h \to 0} \frac{1}{\Gamma(\alpha) h^{\alpha}} \sum_{k=0}^{(t-a)/h} \frac{\Gamma(\alpha+k)}{\Gamma(k+1)} f(t-kh). \tag{2} $$

One can observe that by introducing the notion of fractional order operator ${}_aD_t^{\alpha} f(t)$ the differentiator and integrator can be unified.

Another useful tool is the Laplace transform. The Laplace transform of an n-th derivative ($n \in R_+$) of a signal $x(t)$ relaxed at $t = 0$ is given by: $L\{D^n x(t)\} = s^n X(s)$. So, a fractional order differential equation, provided both the signal $u(t)$ and $y(t)$ are relaxed at $t = 0$, can be expressed in a transfer function form

$$ G(s) = \frac{a_1 s^{\alpha 1} + \alpha_2 s^{\alpha 2} + \ldots + a_{mA} s^{\alpha_{mA}}}{b_1 s^{\beta 1} + b_2 s^{\beta 2} + \ldots + b_{mB} s^{\beta_{mA}}} \,, \tag{3} $$

where $(a_m, b_m) \in R^2$, $(\alpha_m, \beta_m) \in R_+^2$, $\forall (m \in N)$.

Thorough expositions of these subjects may be found in [22] and [50].

2.2. Fractional order PI$^{\lambda}$D$^{\mu}$A controller

The parallel form of the fractional order PI$^{\lambda}$D$^{\mu}$A controller having an integrator of order λ and a differentiator of order μ, is defined as follows:

$$C(s) = \frac{U(s)}{E(s)} = k_p + \frac{k_i}{s^{\lambda}} + k_d s^{\mu} + k_a s^2, \quad (\lambda\mu > 0), \tag{4}$$

where K_p is the proportional gain, K_i is the integration gain, K_d is the derivative gain; K_a is the acceleration gain, λ and μ are the integral and derivative orders, respectively, satisfying $0 < \lambda, \mu < 2$, Fig. 1 shows the block diagram of the parallel form of the fractional order PI$^{\lambda}$D$^{\mu}$A controller. The time domain control signal is represented by:

$$u(t) = K_p e(t) + K_i D^{-\lambda} e(t) + K_d D^{\mu} e(t) + K_a D^2 e(t). \tag{5}$$

For a classical PIDA controller, K_p = proportional gain, K_i = integral gain, K_d = derivative gain, K_a = acceleration gain, λ and μ are both equal to 1. The interest of our proposed fractional order PI$^{\lambda}$D$^{\mu}$A control structure is justified by a better flexibility, since it has two more parameters which are the fractional integration action order λ and the fractional differentiation action order μ. These parameters can be used to fulfil additional specifications for the design or other interesting requirements for the controlled system, than in the case of a classical PIDA control structure ($\lambda = 1$, $\mu = 1$).

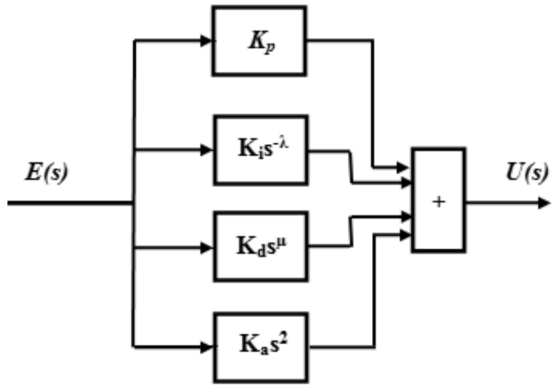

Figure 1: Block diagram of the fractional order PI$^{\lambda}$D$^{\mu}$A controller

2.3. Bode's ideal transfer function

An ideal open-loop transfer function is proposed in [30], that is

$$L(s) = \left(\frac{\omega_c}{s}\right)^{\alpha}, \quad \alpha \in R, \tag{6}$$

where ω_c is the gain crossover frequency, that is $|L(s)| = 1$, and $0 < \alpha < 2$ is a real.

The parameter α determines both the slope of the magnitude curve on Bode plot and the phase margin of the system. In the Bode diagrams, the amplitude of $L(s)$ is a straight line of constant slope -20α dB/dec and its phase curve is a horizontal line at $\frac{\alpha\pi}{2}$ rad which indicates the Bode's ideal transfer function $L(s)$ possesses strong robustness against gain variation. It means that the variation of the process gain only changes the crossover frequency ω_c but maintains the phase margin constant $\pi\left(1-\frac{\alpha}{2}\right)$ rad.

Figure 2 and Fig. 3 show a feedback system with Bode's ideal transfer function in the forward path and Bode diagrams of amplitude and phase of $L(s)$.

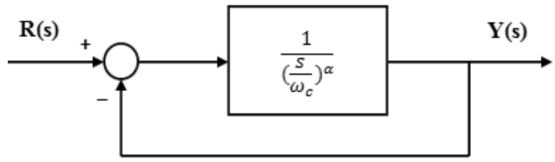

Figure 2: Feedback system with Bode's ideal transfer function in the forward path

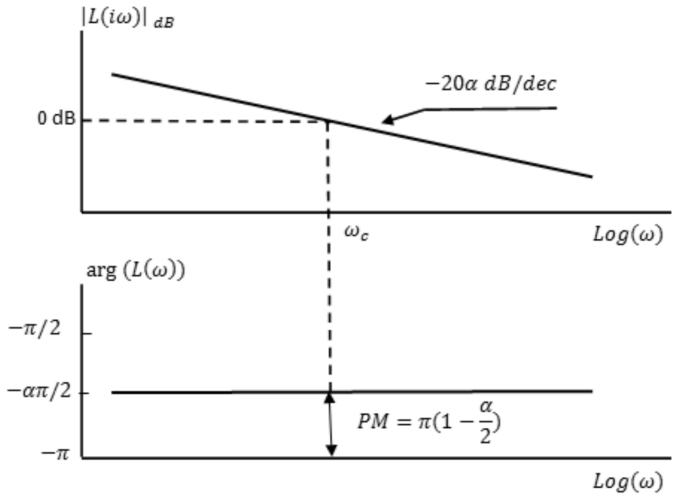

Figure 3: Bode diagrams of amplitude and phase of $L(s)$ for $0 < \alpha < 2$

The choice of $L(s)$ as open loop transfer function also gives an ideal closed loop transfer function under a unit feedback defined as follow:

$$F(s) = \frac{1}{1+\left(\frac{s}{\omega_c}\right)^{\alpha}} \tag{7}$$

with infinite gain margin and constant phase margin.

2.4. Problem statement

In this work, as shown in Fig. 4, we consider the negative unity feedback closed loop system of the form

$$W(s) = \frac{Y(s)}{R(s)} = \frac{C(s)G_{p(s)}}{1 + C(s)G_p(s)}, \tag{8}$$

where $C(s)$ is the fractional order PI$^{\lambda}$D$^{\mu}$A controller and $G_p(s)$ is the plant under control.

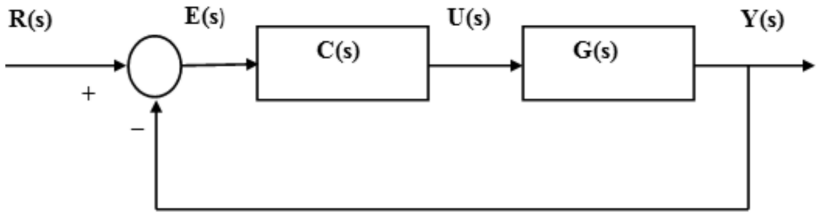

Figure 4: Classical unity feedback control system

The design problem of this feedback control system is to find the fractional order controller $C(s)$ of Equation (4) to guarantee that the closed loop transfer function $W(s)$ behaves in a given frequency band as a desired reference model whose transfer function is the Bode's ideal transfer function given by

$$F_d(s) = \frac{1}{1 + \left(\frac{s}{\omega_u}\right)^m}. \tag{9}$$

This function is considered as the closed loop transfer function of the unity feedback control of Fig. 4 whose open loop transfer function is given by

$$L_d(s) = \left(\frac{\omega_u}{s}\right)^m. \tag{10}$$

The two parameters m and ω_u are chosen such that the above desired $F_d(s)$ system meets the dynamic performance requirements of the projected feedback control system. If these performance requirements of the projected feedback control system can be given in terms of the unity gain crossover frequency ω_c and the phase margin ϕm, the two parameters m and ω_u are obtained as follows:

- $\omega_u = \omega_c$ (the unity gain crossover frequency of the projected feedback control system),
- $m = 2[1 - (\phi m/\pi)]$ (ϕm is the phase margin of the projected feedback control system).

Therefore, the design objective is simply summarized to the tuning of the six parameters K_p, K_i, K_d, K_a, λ and μ of the fractional order PI$^{\lambda}$D$^{\mu}$A controller to satisfy the condition $W(s) = F_d(s)$ in a given frequency band around the unity gain crossover frequency $\omega_c = \omega_u$.

The above two functions $W(s)$ and $F_d(s)$ can be represented by Taylor–Maclaurin series expansion in $s$at the unity gain crossover frequency $s = \omega_u$ as follows:

$$W(s) = W(\omega_u) + (s-\omega_u)\,W^{(1)}(\omega_u) + \frac{(s-\omega_u)^2}{2!}W^{(2)}(\omega_u) + \ldots + \frac{(s-\omega_u)^i}{i!}W^{(i)}(\omega_u) + \ldots, \tag{11}$$

$$F_d(s) = F_d(\omega_u) + (s-\omega_u)\,F_d^{(1)}(\omega_u) + \frac{(s-\omega_u)^2}{2!}F_d^{(2)}(\omega_u) + \ldots + \frac{(s-\omega_u)^i}{i!}F_d^{(i)}(\omega_u) + \ldots, \tag{12}$$

where $W^{(i)}(\omega_u)$ and $F_d^{(i)}(\omega_u)$ are, respectively, the i-th derivatives of the functions $W(s)$ and $F_d(s)$ with respect to s at ω_u.

Because our goal is the design of the fractional order PI$^{\lambda}$D$^{\mu}$A controller to satisfy the condition $W(s) \cong F_d(s)$, the truncation of the above series up to the sixth order term is then sufficient to set up six independent equations to tune the six parameters K_p, K_i, K_d, K_a, λ and μ of the fractional order PI$^{\lambda}$D$^{\mu}$A controller. Therefore, from Equations (11) and (12) we have

$$\begin{cases} W(\omega_u) = F_d(\omega_u), \\ W^{(1)}(\omega_u) = F_d^{(1)}(\omega_u), \\ W^{(2)}(\omega_u) = F_d^{(2)}(\omega_u), \\ W^{(3)}(\omega_u) = F_d^{(3)}(\omega_u), \\ W^{(4)}(\omega_u) = F_d^{(4)}(\omega_u), \\ W^{(5)}(\omega_u) = F_d^{(5)}(\omega_u). \end{cases} \tag{13}$$

Therefore, the proposed feedback control design sums up to the tuning of the parameters of the fractional order PI$^{\lambda}$D$^{\mu}$A controller in order to satisfy all the six equalities of Equation (13).

3. The proposed method

3.1. Description of the design method

The description of the proposed fractional order PI$^{\lambda}$D$^{\mu}$A controller design method is given as following.

Step 1

Let $\theta_i = W^{(i)}(\omega_u) = F_d^{(i)}(\omega_u)$, for $0 \leqslant i \leqslant 5$, so from Equation (8) and the desired reference model function of Equation (9), we have

$$\begin{aligned}
\theta_0 &= W(\omega_u) = F_A(\omega_u) = \frac{1}{2}\,,\\
\theta_1 &= W^{(1)}(\omega_u) = F_d^{(1)}(\omega_u) = -\frac{m}{4\omega_u}\,,\\
\theta_2 &= W^{(2)}(\omega_u) = F_d^{(2)}(\omega_u) = \frac{m}{4\omega_u^2}\,,\\
\theta_3 &= W^{(3)}(\omega_u) = F_d^{(3)}(\omega_u) = \frac{m(m^2-4)}{8\omega_u^3}\,,\\
\theta_4 &= W^{(4)}(\omega_u) = F_d^{(4)}(\omega_u) = -\frac{3m(m^2-2)}{4\omega_u^4}\,,\\
\theta_5 &= W^{(5)}(\omega_u) = F_d^{(5)}(\omega_u) = \frac{m(-2m^4+35m^2-48)}{8m^5}\,.
\end{aligned} \tag{14}$$

Hence, the numerical values of the variables θ_i, for $0 \leqslant i \leqslant 5$, are calculated from the given numerical values of the parameters m and ω_u.

Let $X_i = C^{(i)}(\omega_u)$, for $0 \leqslant i \leqslant 5$, the i-th derivative of the fractional order PI$^{\lambda}$D$^{\mu}$A controller transfer function $C(s)$ with respect to the variable s at $s = \omega_u$. Therefore, from the fractional order PI$^{\lambda}$D$^{\mu}$A controller transfer function of Equation (4), we have

$$\begin{aligned}
X_i &= C^{(i)}(\omega_u),\\
X_0 &= C(\omega_u) = K_p + K_i\omega_u^{-\lambda} + K_d\omega_u^{\mu} + K_a\omega_u^2\,,\\
X_1 &= C^{(1)}(\omega_u) = \frac{-\lambda K_I}{\omega_u}\omega_u^{-\lambda} + \frac{\mu K_D}{\omega_u}\omega_u^{\mu} + 2K_A\omega_u\,,\\
X_2 &= C^{(2)}(\omega_u) = \frac{\lambda(\lambda+1)K_I}{\omega_u^2}\omega_u^{-\lambda} + \frac{\mu(\mu-1)K_D}{\omega_u^2}\omega_u^{\mu} + 2K_A\,,\\
X_3 &= C^{(3)}(\omega_u) = \frac{-\lambda(\lambda+1)(\lambda+2)K_I}{\omega_u^3}\omega_u^{-\lambda} + \frac{\mu(\mu-1)(\mu-2)K_D}{\omega_u^3}\omega_u^{\mu}\,,
\end{aligned} \tag{15}$$

[equation (15) cont.]

$$X_4 = C^{(4)}(\omega_u) = \frac{\lambda(\lambda+1)(\lambda+2)(\lambda+3)K_I}{\omega_u^4}\omega_u^{-\lambda} + \frac{\mu(\mu-1)(\mu-2)(\mu-3)K_D}{\omega_u^4}\omega_u^{\mu},$$

$$X_5 = C^{(5)}(\omega_u) = \frac{-\lambda(\lambda+1)(\lambda+2)(\lambda+3)(\lambda+4)K_I}{\omega_u^5}\omega_u^{-\lambda} + \frac{\mu(\mu-1)(\mu-2)(\mu-3)K_D}{\omega_u^4}\omega_u^{\mu}.$$

Step 2

Let $G_{St}(s)$ the Laplace transform of the step response $g_{St}(t)$ of the process, so $G_{St}(s)$ is given by the following:

$$G_{St}(s) = \int_0^\infty g_{St}(t)e^{-st}\,\mathrm{d}t. \tag{16}$$

The two functions e^{-st} and $G_{St}(s)$ of Equation (16) can be represented by Taylor–Maclaurin series expansion in s at $s = \omega_u$ as follows:

$$G_{St}(s) = \int_0^\infty g_{St}(t)e^{-st}\,\mathrm{d}t + (s-\omega_u)\left\{\int_0^\infty (-t g_{St}(t)e^{-\omega_u t})\,\mathrm{d}t\right\} + \frac{(s-\omega_u)^2}{2!}\left\{\int_0^\infty (t^2 g_{St}(t)e^{-\omega_u t})\,\mathrm{d}t\right\} + \frac{(s-\omega_u)^3}{3!}\left\{\int_0^\infty (-t^3 g_{St}(t)e^{-\omega_u t})\,\mathrm{d}t\right\} + \ldots, \tag{17}$$

$$G_{St}(s) = G_{St}(\omega_u) + (s-\omega_u)\,G_{St}^{(1)}(\omega_u) + \frac{(s-\omega_u)^2}{2!}G_{St}^{(2)}(\omega_u) + \frac{(s-\omega_u)^3}{3!}G_{St}^{(3)}(\omega_u) + \ldots, \tag{18}$$

where $G_{St}^{(i)}(\omega_u)$, for $0 \leqslant i \leqslant 5$, is the i-th derivative of the transfer function $G_{St}(s)$ with respect to s at $s = \omega_u$. We denote $S_i = G_{St}^{(i)}(\omega_u)$, for $0 \leqslant i \leqslant 5$, so from

Equations (17) and (18) we have

$$
\begin{aligned}
S_0 &= G_{St}(s) = \int_0^{\infty} g_{St}(t)e^{-st}\,\mathrm{d}t\,,\\
S_1 &= G_{St}^{(1)}(\omega_u) = \left\{\int_0^{\infty}\left(-tg_{St}(t)e^{-\omega_u t}\right)\mathrm{d}t\right\},\\
S_2 &= G_{St}^{(2)}(\omega_u) = \left\{\int_0^{\infty}\left(t^2 g_{St}(t)e^{-\omega_u t}\right)\mathrm{d}t\right\},\\
S_3 &= G_{St}^{(3)}(\omega_u) = \left\{\int_0^{\infty}\left(-t^3 g_{St}(t)e^{-\omega_u t}\right)\mathrm{d}t\right\},\\
S_4 &= G_{St}^{(4)}(\omega_u) = \left\{\int_0^{\infty}\left(t^4 g_{St}(t)e^{-\omega_u t}\right)\mathrm{d}t\right\},\\
S_5 &= G_{St}^{(5)}(\omega_u) = \left\{\int_0^{\infty}\left(-t^5 g_{St}(t)e^{-\omega_u t}\right)\mathrm{d}t\right\}.
\end{aligned}
\tag{19}
$$

Because $\omega_u > 0$ and the integer $n \geqslant 0$, we have $\lim_{t\to\infty} t^n e^{-\omega_u t} = 0$, $n \geqslant 0$, then the integrals S_i, for $0 \leqslant i \leqslant 5$, of Equation (19) converge and can be calculated numerically using the following formulas:

$$
\begin{aligned}
S_0 &= G_{St}(s) = T\sum_{k=1}^{N} g_{St}(kT)e^{-\omega_u kT},\\
S_1 &= G_{St}^{(1)}(\omega_u) = -T\sum_{k=1}^{N}(kT)g_{St}(kT)e^{-\omega_u kT},\\
S_2 &= G_{St}^{(2)}(\omega_u) = T\sum_{k=1}^{N}(kT)^2 g_{St}(kT)e^{-\omega_u kT},\\
S_3 &= G_{St}^{(3)}(\omega_u) = -T\sum_{k=1}^{N}(kT)^3 g_{St}(kT)e^{-\omega_u kT},
\end{aligned}
\tag{20}
$$

[equation (20) cont.]

$$S_4 = G_{St}^{(4)}(\omega_u) = T\sum_{k=1}^{N}(kT)^4 g_{St}(kT)e^{-\omega_u kT},$$

$$S_5 = G_{St}^{(5)}(\omega_u) = -T\sum_{k=1}^{N}(kT)^5 g_{St}(kT)e^{-\omega_u kT},$$

where T is the sampling period of the step response $g_{St}(t)$ of the process and the number of samples N = integer part of (T_{sim}/T), with T_{sim} being the time of acquisition of the step response which is usually taken higher than the settling time of the process. Therefore, the numerical values of the parameters S_i, for $0 \leqslant i \leqslant 5$, are calculated from the given numerical values of the step response $g_{St}(t)$ of the process and the unity gain crossover frequency ω_u. If the transfer function of the process is available, the parameters S_i can also be calculated directly.

Step 3

The feedback control system open loop transfer function $G_{OL}(s)$ can be obtained from the closed loop transfer function $W(s)$ of Equation (8) as follows:

$$G_{OL}(s) = C(s)G_p(s) = \frac{W(s)}{1 - W(s)}, \tag{21}$$

We can rewrite the above equation as follows:

$$G_{OL}(s) = sC(s)\frac{G_p(s)}{s} = sC(s)G_{St}(s) = \frac{W(s)}{1 - W(s)}, \tag{22}$$

where $G_p(s)/s = G_{St}(s)$ is the Laplace transform of the step response $g_{St}(t)$ of the process of Equation (16). Taking the i-th derivative, for $0 \leqslant i \leqslant 5$, of both sides of Equation (22) with respect to s at $s = \omega_u$ and using the results obtained for the calculations of the terms $W^{(i)}(\omega_u)$, $C^{(i)}(\omega_u)$ and $G_{St}^{(i)}(\omega_u)$ in Equations (14) and (15) from step 1 and Equation (20) from step 2, we then get

$$\begin{aligned}
G_{OL}(\omega_u) &= \omega_u X_0 S_0 = \frac{\theta_0}{1 - \theta_0}, \\
G_{OL}^{(1)}(\omega_u) &= X_0 S_0 + \omega_u X_1 S_0 + \omega_u X_0 S_1 = \frac{\theta_1}{(1 - \theta_1)^2}, \\
G_{OL}^{(2)}(\omega_u) &= 2X_1 S_0 + 2X_0 S_1 + \omega_u X_2 S_0 + 2\omega_u X_1 S_1 + \omega_u X_0 S_2 \\
&= \frac{\theta_2}{(1 - \theta_0)^2} + \frac{2\theta_1^2}{(1 - \theta_0)^3},
\end{aligned} \tag{23}$$

[equation (23) cont.]

$$
\begin{aligned}
G_{OL}^{(3)}(\omega_u) &= 3X_2S_0 + 6X_1S_1 + 3X_0S_2 + \omega_u X_3S_0 + \omega_u X_3S_0 + 3\omega_u X_2S_1 + 3\omega_u X_1S_2 \\
&= \frac{\theta_3}{(1-\theta_0)^2} + \frac{6\theta_1\theta_2}{(1-\theta_0)^3} + \frac{6\theta_1^3}{(1-\theta_0)^4}, \\
G_{OL}^{(4)}(\omega_u) &= 4X_3S_0 + 12X_2S_1 + 12X_1S_2 + 4X_0S_3 + \omega_u X_4S_0 + \omega_u X_0S_4 \\
&\quad + 4\omega_u X_3S_1 + 4\omega_u X_1S_3 + 6\omega_u X_2S_2 \\
&= \frac{\theta_4}{(1-\theta_0)^2} + \frac{6\theta_2^2 + 8\theta_1\theta_3}{(1-\theta_0)^3} + \frac{36\theta_1^2\theta_2}{(1-\theta_0)^4} + \frac{24\theta_1^4}{(1-\theta_0)^5}, \\
G_{OL}^{(5)}(\omega_u) &= 5X_4S_0 + 20X_3S_1 + 30X_2S_2 + 20X_1S_3 + 5X_0S_4 + \omega_u X_5S_0 \\
&\quad + 5\omega_u X_4S_1 + 5\omega_u X_1S_4 + \omega_u X_0S_5 + 10\omega_u X_3S_2 + 10\omega_u X_2S_3 \\
&= \frac{\theta_5}{(1-\theta_0)^2} + \frac{10\theta_1\theta_4 + 20\theta_2\theta_3}{(1-\theta_0)^3} + \frac{90\theta_1\theta_2^2 + 60\theta_1^2\theta_3}{(1-\theta_0)^4} + \frac{240\theta_1^3\theta_2}{(1-\theta_0)^5} + \frac{120\theta_1^5}{(1-\theta_0)^6}.
\end{aligned}
$$

Then, the numerical values of the terms $G_{OL}^{(i)}(\omega_u)$ for $0 \leqslant i \leqslant 5$ are calculated from the obtained numerical values of the variables θ_i of Equation (14) from step 1.

Step 4

Because the numerical values of the terms $G_{OL}^{(i)}(\omega_u)$, of the variables S_i, for $0 \leqslant i \leqslant 5$, and of the unity gain crossover frequency ω_u are known, the variables X_i, for $0 \leqslant i \leqslant 5$, can be derived and calculated from Equation (23) as follows:

$$
\begin{aligned}
X_0 &= \frac{G_o(\omega_u)}{\omega_u S_0}, \\
X_1 &= \frac{1}{\omega_u S_0}\Big(G_o^{(1)}(\omega_u) - X_0S_0 - \omega_u X_0S_1\Big), \\
X_2 &= \frac{1}{\omega_u S_0}\Big(G_o^{(2)}(\omega_u) - 2X_1S_0 - 2X_0S_1 - 2\omega_u X_1S_1 - \omega_u X_0S_2\Big), \\
X_3 &= \frac{1}{\omega_u S_0}\Big(G_o^{(3)}(\omega_u) - 3X_2S_0 - 6X_1S_1 - 3X_0S_2 - \omega_u X_0S_3 - 3\omega_u X_2S_1 \\
&\quad - 3\omega_u X_1S_2\Big), \\
X_4 &= \frac{1}{\omega_u S_0}\Big(G_o^{(4)}(\omega_u) - 4X_3S_0 - 12X_2S_1 - 12X_1S_2 - 4X_0S_3 - \omega_u X_0S_4 \\
&\quad - 4\omega_u X_3S_1 - 4\omega_u X_1S_3 - 6\omega_u X_2S_2\Big),
\end{aligned}
\tag{24}
$$

[equation (24) cont.]

$$X_5 = \frac{1}{\omega_u S_0}\Big(G_o^{(5)}(\omega_u) - 5X_4S_0 - 20X_3S_1 - 30X_2S_2 - 20X_1S_3 - 5X_0S_4 \\ - \omega_u X_5S_0 - 5\omega_u X_4S_1 - 5\omega_u X_1S_4 - \omega_u X_0S_5 - 10\omega_u X_3S_2 - 10\omega_u X_2S_3\Big).$$

Step 5

Let us define the following variables:

$$\begin{aligned} Q_1 &= \frac{-\lambda K_I}{\omega_u}\omega_u^{-\lambda}, \\ Q_2 &= \frac{\mu K_D}{\omega_u}\omega_u^{\mu}, \\ Q_3 &= 2K_a\omega_u^{\mu}. \end{aligned} \tag{25}$$

Then, Equation (15) can be rewritten as follows:

$$\begin{aligned} X_0 &= K_p + K_i\omega_u^{-\lambda} + K_d\omega_u^{\mu} + K_a\omega_u^2, \\ X_1 &= Q_1 + Q_2 + Q_3, \\ X_2 &= -(\lambda+1)\frac{Q_1}{\omega_u} + (\mu-1)\frac{Q_2}{\omega_u} + \frac{Q_3}{\omega_u}, \\ X_3 &= (\lambda+1)(\lambda+2)\frac{Q_1}{\omega_u^2} + (\mu-1)(\mu-2)\frac{Q_2}{\omega_u^2}, \\ X_4 &= -(\lambda+1)(\lambda+2)(\lambda+3)\frac{Q_1}{\omega_u^3} + (\mu-1)(\mu-2)(\mu-3)\frac{Q_2}{\omega_u^3}, \\ X_5 &= (\lambda+1)(\lambda+2)(\lambda+3)(\lambda+4)\frac{Q_1}{\omega_u^4} + (\mu-1)(\mu-2)(\mu-3)(\mu-4)\frac{Q_2}{\omega_u^4}. \end{aligned} \tag{26}$$

Let us also define the variables Z_1, Z_2, Z_3 and Z_4 as follows:

$$\begin{aligned} Z_1 &= X_1 + \omega_u X_2, \\ Z_2 &= X_1 + 3\omega_u X_2 + \omega_u^2 X_3, \\ Z_3 &= X_1 + 7\omega_u X_2 + 6\omega_u^2 X_3 + \omega_u^3 X_4, \\ Z_4 &= X_1 + 15\omega_u X_2 + 25\omega_u^2 X_3 + 10\omega_u^3 X_4 + \omega_u^4 X_5. \end{aligned} \tag{27}$$

The numerical values of the variables Z_i, for $1 \leqslant i \leqslant 4$ can be calculated from the values of the variables X_i, for $0 \leqslant i \leqslant 5$, and the unity gain crossover

frequency ω_u. Now, combining Equations (26) and (27) we get the following:

$$\begin{aligned}
X_0 &= K_p + K_i\omega_u^{-\lambda} + K_d\omega_u^{\mu} + K_a\omega_u^2\,,\\
X_1 &= Q_1 + Q_2 + Q_3\,,\\
Z_1 &= -\lambda Q_1 + \mu Q_2 + 2Q_3\,,\\
Z_2 &= \lambda^2 Q_1 + \mu^2 Q_2 + 4Q_3\,,\\
Z_3 &= -\lambda^3 Q_1 + \mu^3 Q_2 + 8Q_3\,,\\
Z_4 &= \lambda^4 Q_1 + \mu^4 Q_2 + 16Q_3\,.
\end{aligned} \tag{28}$$

Let us now define the variables V_1, V_2, V_3 and V_4 as follows:

$$\begin{aligned}
V_1 &= -2X_1 + Z_1 = -(2+\lambda)Q_1 + (\mu-2)Q_2\,,\\
V_2 &= -2Z_1 + Z_2 = \lambda(2+\lambda)Q_1 + \mu(\mu-2)Q_2\,,\\
V_3 &= -2Z_2 + Z_3 = -\lambda^2(2+\lambda)Q_1 + \mu^2(\mu-2)Q_2\,,\\
V_4 &= -2Z_3 + Z_4 = \lambda^3(2+\lambda)Q_1 + \mu^3(\mu-2)Q_2\,.
\end{aligned} \tag{29}$$

With some manipulations of Equation (26) and (29), we can easily get

$$\begin{aligned}
X_0 &= K_p + K_i\omega_u^{-\lambda} + K_d\omega_u^{\mu} + K_a\omega_u^2\,,\\
X_1 &= Q_1 + Q_2 + Q_3\,,\\
\lambda V_1 + V_2 &= (\lambda+\mu)(\mu-2)Q_2\,,\\
\lambda V_2 + V_3 &= \mu(\lambda+\mu)(\mu-2)Q_2\,,\\
\lambda V_3 + V_4 &= \mu^2(\lambda+\mu)(\mu-2)Q_2\,.
\end{aligned} \tag{30}$$

Step 6

From the last three equalities of Equation (30), we can derive the following equation:

$$\frac{\lambda V_2 + V_3}{\lambda V_1 + V_2} = \frac{\lambda V_3 + V_4}{\lambda V_2 + V_3} = \mu\,. \tag{31}$$

Then, from the two first terms of Equation (31) we get

$$(\lambda Z_{22} + Z_{33})^2 - (\lambda Z_{11} + Z_{22})\,(\lambda Z_{33} + Z_{44}) = 0. \tag{32}$$

This leads to a second-order equation in the parameter λ as follows:

$$\lambda^2\left(Z_{22}^2 - Z_{11}Z_{33}\right) + \lambda\,(2Z_{22}Z_{33} - Z_{11}Z_{44} - Z_{22}Z_{33}) + \left(Z_{33}^2 - Z_{22}Z_{44}\right) = 0. \tag{33}$$

By solving this second-order equation a convenient numerical value of the parameter λ can be chosen. Then, the other remaining parameters K_p, K_i, K_d, K_a,

λ and μ will be successively obtained. The first to be calculated is the parameter μ from Equation (31) as follows:

$$\frac{\lambda Z_{22} + Z_{33}}{\lambda Z_{11} + Z_{22}} = \frac{\lambda Z_{33} + Z_{44}}{\lambda Z_{22} + Z_{33}} = \mu \,. \tag{34}$$

From Equation (29) and (30), the parameters Q_1, Q_2 and Q_3 are given as follows:

$$\begin{aligned} Q_2 &= \frac{\lambda V_1 + V_2}{(\lambda + \mu)(\mu - 2)} \,, \\ Q_1 &= \frac{-V_1 + (\mu - 2)Q_2}{(2 + \lambda)} \,, \\ Q_3 &= X_1 - Q_1 - Q_2 \,, \end{aligned} \tag{35}$$

Therefore, from Equations (25) and (35) the three parameters K_i, K_d and K_a are calculated as follows:

$$\begin{aligned} K_i &= \frac{-Q_1 \omega_u}{\lambda \omega_u^{-\lambda}} \,, \\ K_d &= \frac{Q_2 \omega_u}{\mu \omega_u^{\mu}} \,, \\ K_a &= \frac{Q_3}{2\omega_u} \,. \end{aligned} \tag{36}$$

Finally, the parameter K_p can be obtained from Equation (30) as follows:

$$K_p = X_0 - K_i \omega_u^{-\lambda} + K_d \omega_u^{\mu} + K_a \omega_u^2 \,. \tag{37}$$

3.2. Design procedure of fractional order PI$^{\lambda}$D$^{\mu}$A controller

For the tuning of the parameters K_p, K_i, K_d, K_a, λ and μ of the fractional order PI$^{\lambda}$D$^{\mu}$A controller of the feedback control system of Fig. 4 so that its closed loop transfer function behaves like the transfer function of a desired reference fractional model of Equation (9) that meets the requirements and the specifications of the projected feedback control system, we will follow the next steps.

3.2.1. Inputs

We have the following inputs:

- the crossover frequency ω_u and the fractional order m of the desired reference model,
- the values of the step response of the process $g_{St}(kT)$, for $0 \leqslant k \leqslant N$, where N = integer part of (T_{sim}/T), with T_{sim} being the time of acquisition and T is the sampling period of the step response of the process.

3.2.2. Design algorithm

Procedures of the proposed fractional order PI$^{\lambda}$D$^{\mu}$A controller design method are given as following:

Step 1: Calculation of the variables θi, for $0 \leqslant i \leqslant 5$ from Equation (14);

Step 2: Calculation of the variables Si, for $0 \leqslant i \leqslant 5$ from Equation (19);

Step 3: Calculation of the terms $G_{OL}^{(i)}(\omega_u)$, for $0 \leqslant i \leqslant 5$ from Equation (23);

Step 4: Calculation of the variables Xi, for $0 \leqslant i \leqslant 5$ from Equation (24);

Step 5: Calculation of the variables Zi, for $1 \leqslant i \leqslant 4$ from Equation (27);

Step 6: Calculation of the variables Vi, for $1 \leqslant i \leqslant 4$ from Equation (29);

Step 7: Calculation of the fractional order PI$^{\lambda}$D$^{\mu}$A controller parameters λ, μ, K_i, K_d, K_a and K_p as follows:

- As a suitable solution of the second-order equation of Equation (33) for the parameter λ;
- μ from Equation (34);
- K_i from Equation (36);
- K_d from Equation (36);
- K_a from Equation (36);
- K_p from Equation (37).

4. Simulation results

In this section two illustrative examples will be studied to validate the effectiveness and the usefulness of the proposed fractional order PI$^{\lambda}$D$^{\mu}$A controller design method. The controller design will be considered for two real world system models given in [15].

4.1. DC servo motor

The transfer function of DC servo motor is as follows:

$$G(s) = \frac{\theta(s)}{V_a(s)} = \frac{2}{s^3 + 12s^2 + 20.02s}. \tag{38}$$

Here the Angular displacement $\theta(s)$ is considered the output, and the armature voltage $V_a(s)$ is considered the input.

The desired specifications of induction motor are as follows [15]:

– Percentage overshoot (P.O.) $\leqslant 5\%$.

– Settling time (t_s) $\leqslant 2$ sec.

These performance requirements are satisfied by the reference model whose transfer function is given as follows:

$$G_d(s) = \frac{1}{1+\left(\frac{s}{w_u}\right)^m} = \frac{1}{1+\left(\frac{s}{3.5}\right)^{1.0556}}, \tag{39}$$

whose open loop transfer function is $\left(\frac{s}{3.5}\right)^{-1.0556}$, with unity gain crossover frequency $\omega_u = 3.5$ rad/sec and the phase margin $\phi m = 85°$.

The parameters of fractional order PI$^\lambda$D$^\mu$A controller using our proposed design method and the classical PIDA controller using Jung-Dorf design method are obtained as summarized in Table 1.

Table 1: Comparison of controllers' parameters

Controller	K_p	K_i	K_d	K_a	λ	μ
PIDA [15]	285.818	299.213	94.493	12.177	1	1
PD$^\lambda$D$^\mu$A	41.8653	–31.8591	20.7370	31.7936	–1.9828	1.1281

The designed controller was found to be a fractional order PD$^\lambda$D$^\mu$A controller. This type of controller does not have an equivalent one in the regular classical controllers.

Many methods have been developed to approximate fractional operators in continuous time domain; among them Matsuda, Carlson, General CFE, Oustaloup and Charef are most popular [51]. The transfer function of the fractional order PI$^\lambda$D$^\mu$A controller have been implemented by rational functions through Charef's method [52], in the frequency band $[0.01\omega_u,\ 100\omega_u]$ rad/sec.

Figure 5 shows the Bode diagrams of the open loop transfer functions $C(s)G_p(s)$ of the above feedback control system with the open loop transfer function $\left(\frac{s}{3.5}\right)^{-1.0556}$ of the desired reference fractional order system of (38).

From Fig. 5, we can see that the open loop transfer function of the feedback control system is quite overlapping with the open loop transfer function $\left(\frac{s}{3.5}\right)^{-1.0556}$ of the desired fractional order system of (39) in the frequency band of interest. It means that the unity gain crossover frequency ω_u and the phase margin ϕm of the feedback control system is $\omega_u = 3.5$ rad/sec and $\phi m = 85°$. We note also the flatness of the phase around the crossover frequency $\omega_u = 3.5$ rad/sec.

Figure 6 shows the Bode plots of the closed loop transfer function of the feedback control system with fractional order PI$^\lambda$D$^\mu$A controller and the ideal closed loop transfer function $G_d(s)$.

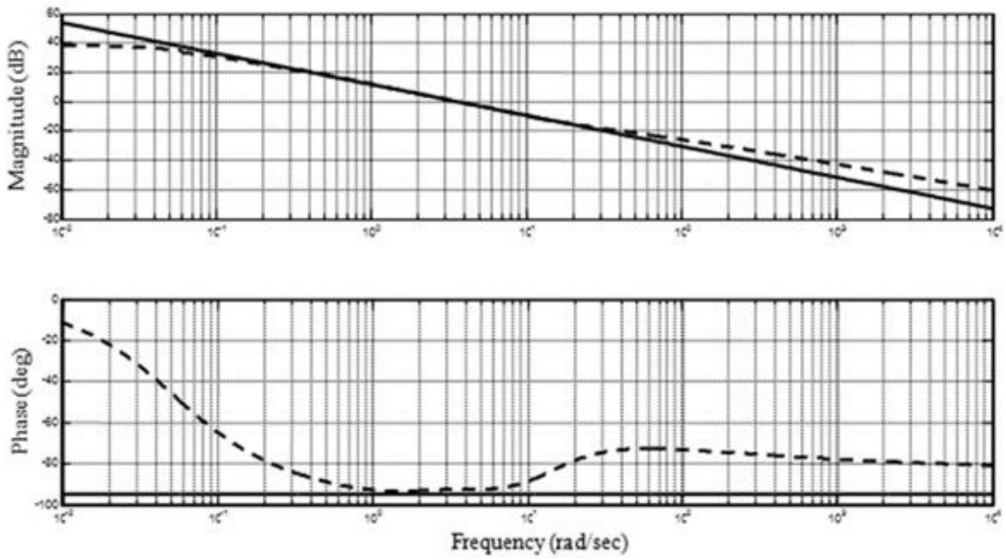

Figure 5: Bode plots of the open loop transfer function $C(s)G_p(s)$ (dashed line) and the desired open loop transfer function $\left(\frac{s}{3.5}\right)^{-1.0556}$ (solid line)

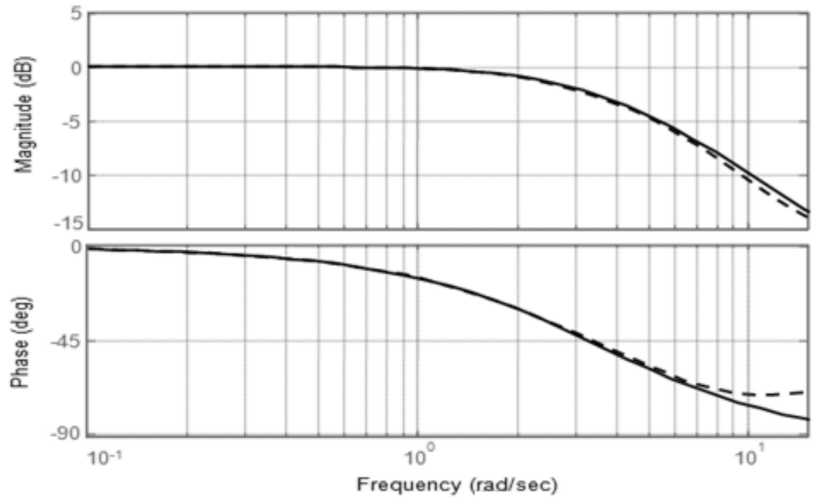

Figure 6: Bode plots of the closed loop transfer function $W(s)$ (dashed line) and the desired closed loop transfer function $G_d(s)$ (solid line)

From Fig. 6, we can easily see that around the unity gain crossover frequency $\omega_u = 3.5$ rad/sec the amplitudes and the phases of the closed loop transfer function of the feedback control system with fractional order PI$^{\lambda}$D$^{\mu}$A controller

and the ideal closed loop transfer function $G_d(s)$ are quiet overlapping. Then, this result shows the effectiveness of the proposed controller design method.

Figure 7 shows the step responses of the closed loop transfer function of the feedback control system with the step response of the desired fractional order system.

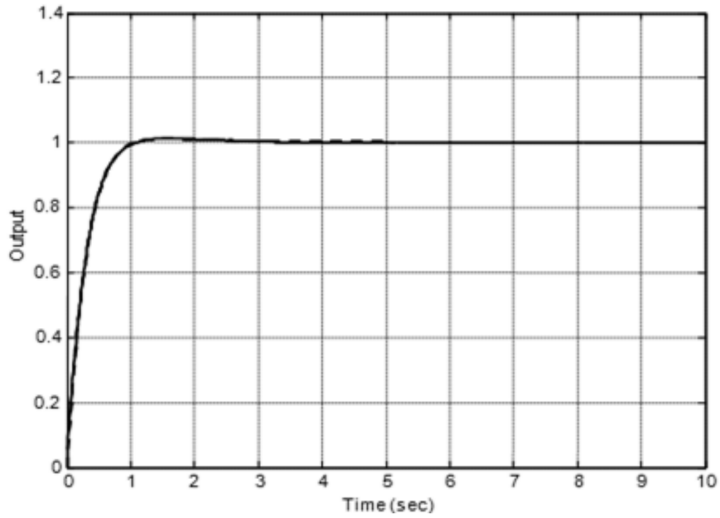

Figure 7: Step responses of the closed loop systems with the open loop transfer function $C(s)G_p(s)$ (dashed line) and the desired fractional order system $G_d(s)$ (solid line)

From Fig. 7, we can easily see that the step response of the feedback control system is equal to the step response of the desired fractional order system.

Figure 8 shows the step response of the closed loop system without controller.

The step responses of the closed loops with fractional order $\mathrm{PI}^{\lambda}\mathrm{D}^{\mu}\mathrm{A}$ controller and of classical PIDA controller are shown in Fig. 9.

Transient response parameters of the two controllers such as percentage overshoot (O%), settling time (St), peak time (Pt) and rise time (Rt) are listed in Table 2.

Table 2: The temporal characteristics for the two controllers

Controller	Rt(0.1:0.9)	St(2%)	O%	Pt
PIDA	0.133	1.270	7.550	0.63
$\mathrm{PI}^{\lambda}\mathrm{D}^{\mu}\mathrm{A}$	0.574	0.890	1.320	1.630

Figure 10 shows the step responses of the closed system with fractional order $\mathrm{PI}^{\lambda}\mathrm{D}^{\mu}\mathrm{A}$ and classical PIDA controllers for different values of the static gain of the process.

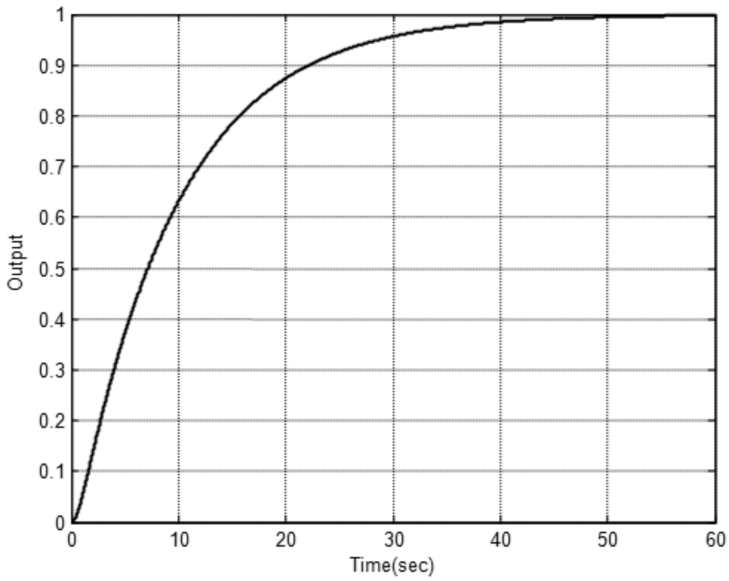

Figure 8: Step responses of the closed loop system without controller

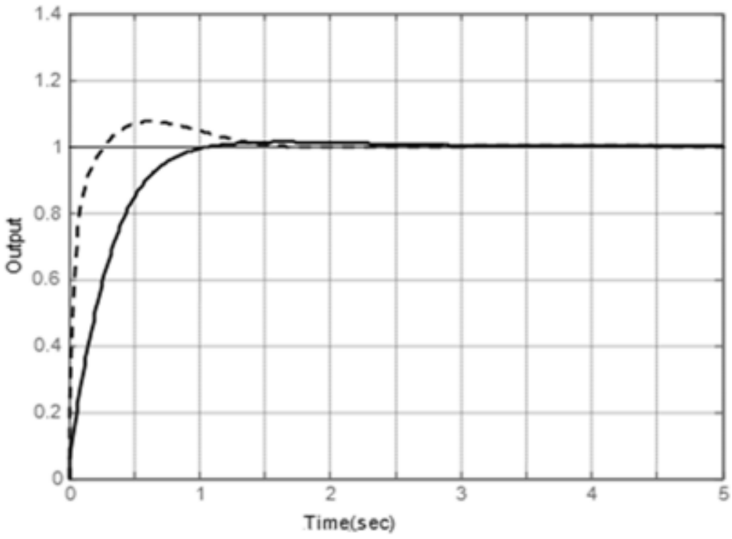

Figure 9: Step response comparison of DC servo motor with fractional order PI$^{\lambda}$D$^{\mu}$A controller (solid line) and classical PIDA controller using Jung-Dorf method (dashed line)

From Fig. 10, we can easily see that the step responses of the closed loop system with fractional order PI$^{\lambda}$D$^{\mu}$A controller for different values of the static gain have the same overshoot which is the iso-damping property. In contrast, the

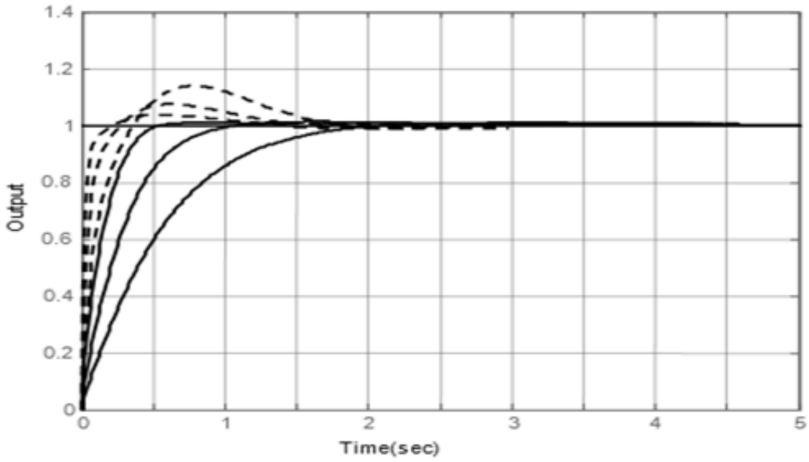

Figure 10: Step response comparison of DC servo motor with fractional order $PI^{\lambda}D^{\mu}A$ controller (solid line) and PIDA controller using Jung-Dorf method (dashed line) for different values of the process gain

overshoot of the step responses of the closed loop system with classical PIDA controller increase when the process gain increases.

To test the robustness of the feedback control system of the DC motor with the proposed fractional order $PI^{\lambda}D^{\mu}A$ controller and with the classical PIDA controller, the variations of the overshoot versus the static gain K ($1 < K < 2.5$) of the transfer function model $G_p(s)$ of (38) is shown in Fig. 11.

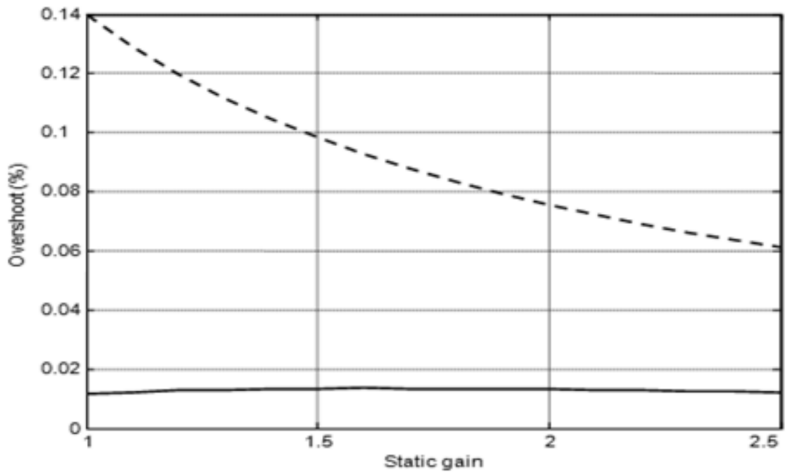

Figure 11: Variations of the overshoot of the feedback control versus static gain with the proposed fractional order $PI^{\lambda}D^{\mu}A$ controller (solid line) and with classical PIDA controller (dashed line)

From Fig. 11, we note that the plot of the overshoot of the feedback control versus the static gain K with the proposed fractional order PI$^{\lambda}$D$^{\mu}$A controller is a horizontal line and with the classical PIDA controller is parabolic line. Hence, we conclude that the feedback control with the proposed fractional order PI$^{\lambda}$D$^{\mu}$A controller is more robust to the variations of the static gain K than with the classical PIDA controller.

4.2. Induction motor

The transfer function of the induction motor is as follows:

$$G(s) = \frac{\theta(s)}{\theta_d(s)} = \frac{168.0436}{s^3 + 25.921s^2 + 168.0436s}. \tag{40}$$

The desired specifications of induction motor are as follows:

– Percentage overshoot (P.O.) $\leqslant 5\%$.

– Settling time (ts) $\leqslant 2$ sec.

These performance requirements are satisfied by the reference model whose transfer function is given as follows:

$$G_d(s) = \frac{1}{1 + \left(\frac{s}{w_u}\right)^m} = \frac{1}{1 + \left(\frac{s}{2}\right)^{1.0556}}, \tag{41}$$

whose open loop transfer function is $\left(\frac{s}{2}\right)^{-1.0556}$, with unity gain crossover frequency $\omega_u = 2$ rad/sec and the phase margin $\phi m = 85°$.

The parameters of fractional order PI$^{\lambda}$D$^{\mu}$A controller using our proposed tuning method, classical PIDA controller using Jung-Dorf method and classical PIDA controller using Kitti's method are obtained as summarized in Table 3.

Table 3: Comparison of controllers' parameters

Controller	K_p	K_i	K_d	K_a	λ	μ
JD-PIDA [15]	12.2384	21.8548	2.4601	0.1268	1	1
K-PIDA [15]	5.6672	9.3764	0.7027	0.0248	1	1
PI$^{\lambda}$D$^{\mu}$A	2.1061	0.0725	0.2461	0.0113	0.7610	1.0911

Figure 12 shows the Bode diagrams of the open loop transfer functions $C(s)G_p(s)$ of the above feedback control system with the open loop transfer function $\left(\frac{s}{2}\right)^{-1.0556}$ of the desired reference fractional order system of (41).

From Fig. 12, we can see that the open loop transfer function of the feedback control system is quite overlapping with the open loop transfer function $\left(\frac{s}{2}\right)^{-1.0556}$

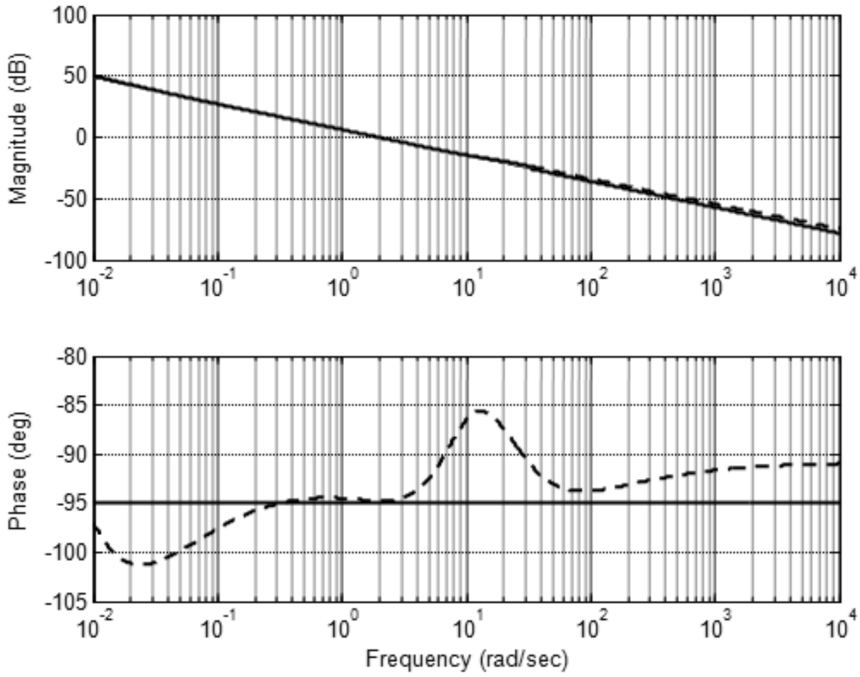

Figure 12: Bode plots of the open loop transfer function $C(s)G_p(s)$ (dashed line) and the desired open loop transfer function $\left(\frac{s}{2}\right)^{-1.0556}$ (solid line)

of the desired fractional order system of (41). It means that the unity gain crossover frequency ω_u and the phase margin ϕm of the feedback control system is $\omega_u = 2$ rad/sec and $\phi m = 85°$. We note also the flatness of the phase around the crossover frequency ω_u.

Figure 13 shows the Bode plots of the closed loop transfer function of the feedback control system with fractional order $\mathrm{PI}^{\lambda}\mathrm{D}^{\mu}\mathrm{A}$ controller and the ideal closed loop transfer function $G_d(s)$.

From Fig. 13, we can easily see that around the unity gain crossover frequency $\omega_u = 2$ rad/sec the amplitudes and the phases of the closed loop transfer function of the feedback control system with fractional order $\mathrm{PI}^{\lambda}\mathrm{D}^{\mu}\mathrm{A}$ controller and the ideal closed loop transfer function $G_d(s)$ are quiet overlapping. Then, this result shows the effectiveness of the proposed controller design method.

Figure 14 shows the step responses of the closed loop transfer function of the feedback control system with the step response of the desired fractional order system.

From Fig. 14, we can easily see that the step response of the feedback control system is equal to the step response of the desired fractional order system.

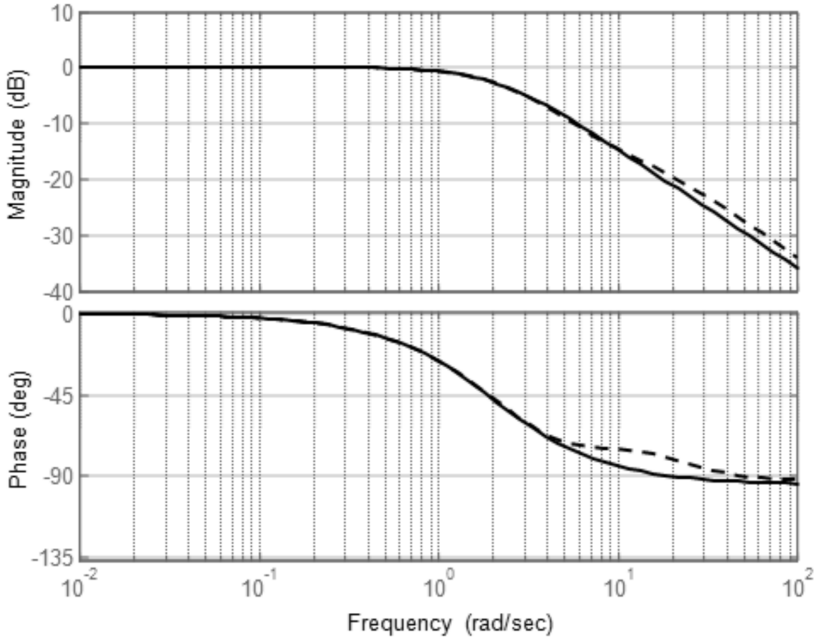

Figure 13: Bode plots of the closed loop transfer function $W(s)$ (dashed line) and the desired closed loop transfer function $G_d(s)$ (solid line)

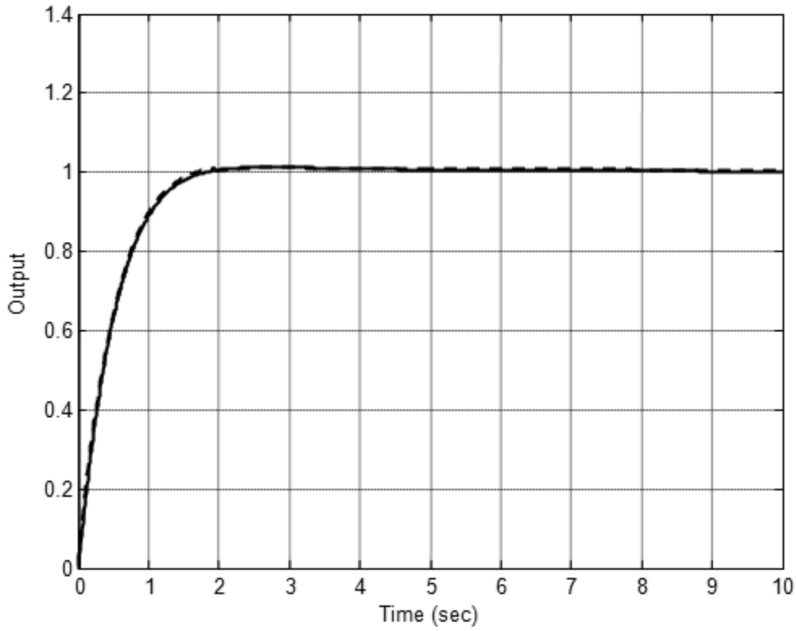

Figure 14: Step responses of the closed loop systems with the open loop transfer function $C(s)G_p(s)$ (dashed line) and the desired fractional order system $G_d(s)$ (solid line)

The step responses of the closed loops with the proposed fractional order $PI^{\lambda}D^{\mu}A$ controller and classical PIDA controllers using Jung-Dorf and Kitti's methods are shown in Fig. 15.

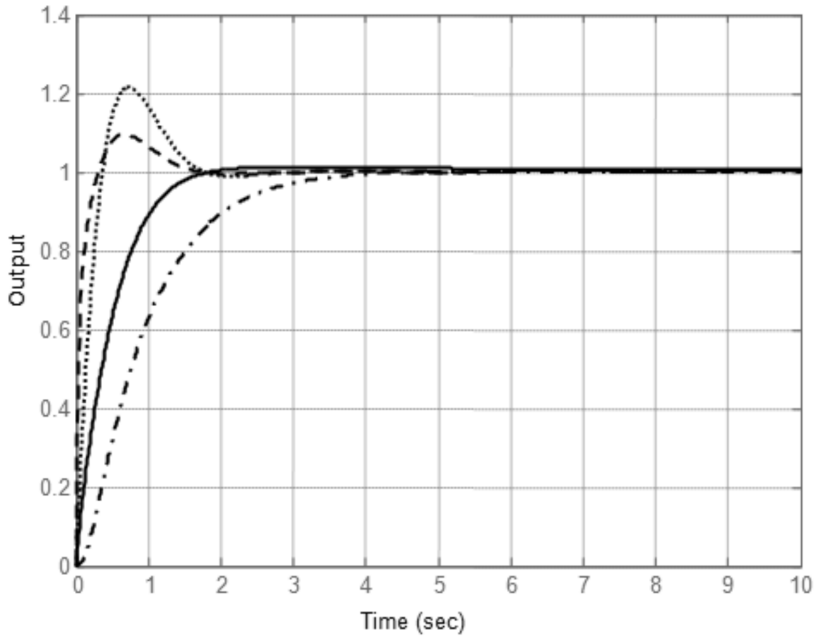

Figure 15: Step response comparison of induction motor without controller (dash-dotted line), with fractional order $PI^{\lambda}D^{\mu}A$ (solid line), PIDA Controllers using Jung-Dorf method (dashed line) and Kitti's method (dotted)

Transient response parameters of the three controllers such as percentage overshoot, settling time peak time and rise time are listed in Table 4.

Table 4: The temporal characteristics for the three controllers

Controller	Rt(0.1:0.9)	St(2%)	O%	Pt
JD-PIDA [15]	0.182	1.38	9.48	0.67
K-PIDA [15]	0.278	1.59	21.5	0.73
$PI^{\lambda}D^{\mu}A$	0.983	1.520	1.160	2.5

Figure 16 and Fig. 17 show the step responses of the closed system with fractional order $PI^{\lambda}D^{\mu}A$ and classical PIDA controllers for different values of the static gain of the process.

From Fig. 16 and Fig. 17, we can easily see that the step responses of the closed loop system with fractional order $PI^{\lambda}D^{\mu}A$ controller for different values

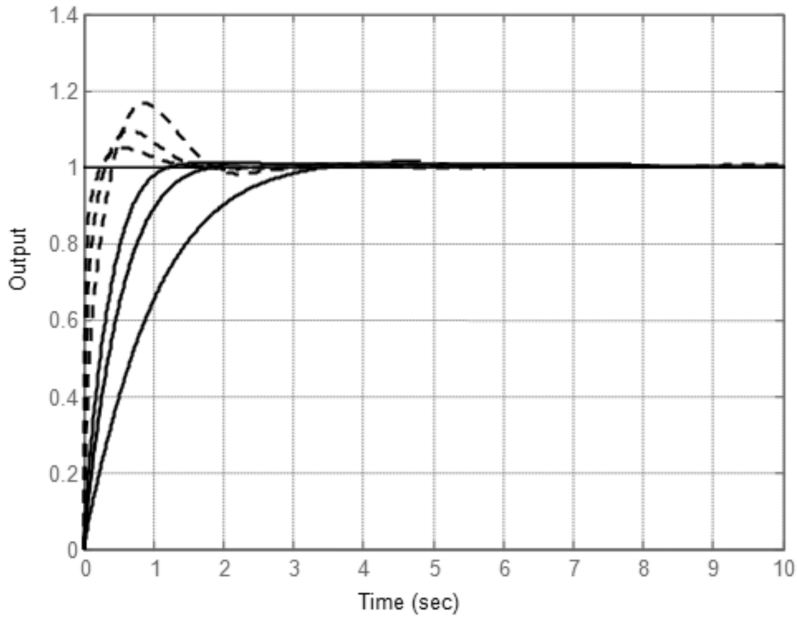

Figure 16: Step responses of the closed loop systems with fractional order PI$^{\lambda}$D$^{\mu}$A (solid line) and PIDA using Jung-Dorf method (dashed line) for different values of the process gain

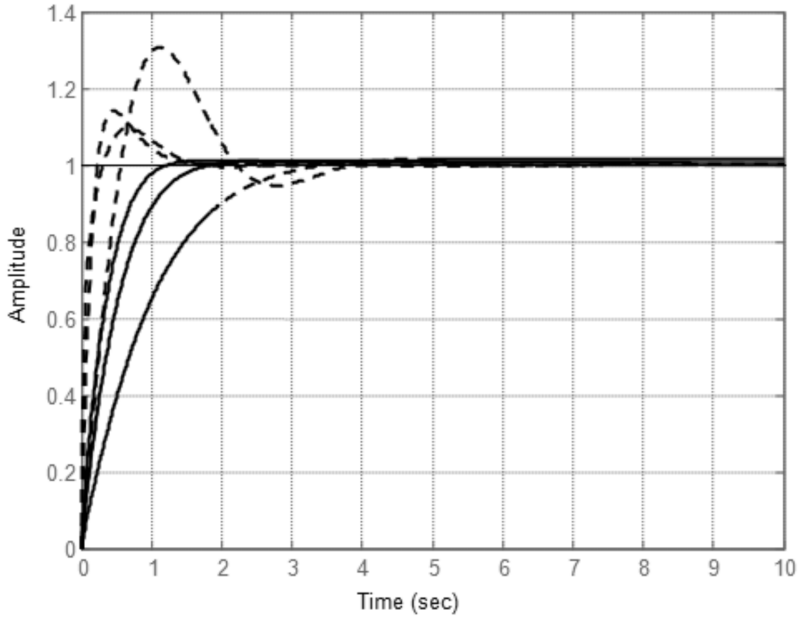

Figure 17: Step responses of the closed loop systems with fractional order PI$^{\lambda}$D$^{\mu}$A (solid line) and PIDA using Kitti's method (dashed line) for different values of the process gain

of the static gain have the same overshoot which is the iso-damping property. In contrast, the overshoot of the step responses of the closed loop system with classical PIDA controller increase when the process gain increases.

To test the robustness of the feedback control system of the induction machine with the proposed fractional order $PI^{\lambda}D^{\mu}A$ controller and with the classical PIDA controllers, the variations of the overshoot versus the static gain K ($100 < K < 220$) the transfer function model $G_p(s)$ of (40) is shown in Fig. 18.

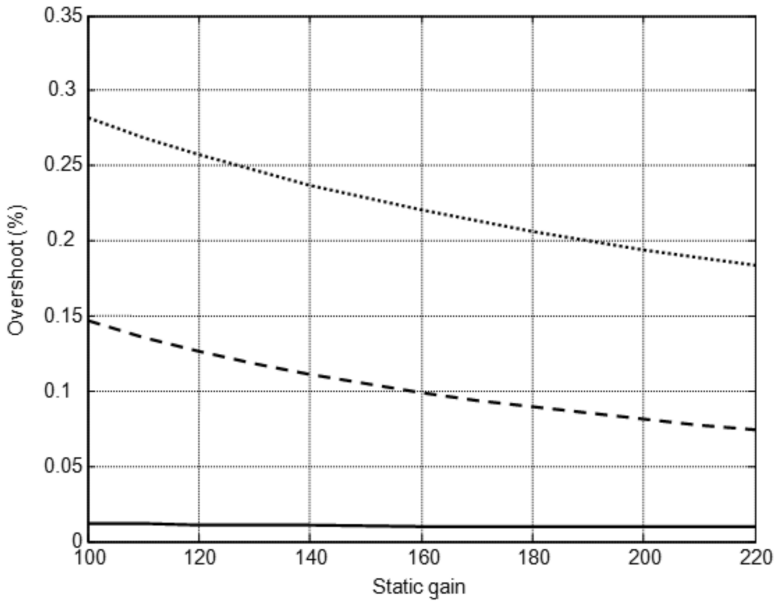

Figure 18: Variations of the overshoot of the feedback control versus static gain with the proposed $PI^{\lambda}D^{\mu}A$ controller (solid line) and with classical PIDA Controllers using Jung-Dorf method (dashed line) and Kitti's method (dotted)

From Fig. 18, we note that the plot of the overshoot of the feedback control versus the static gain K with the proposed fractional order $PI^{\lambda}D^{\mu}A$ controller is a horizontal line and with the classical PIDA controller is parabolic line. Hence, we conclude that the feedback control with the proposed fractional order $PI^{\lambda}D^{\mu}A$ controller is more robust to the variations of the static gain K than with the two classical PIDA controllers.

5. Conclusion

This paper presents a simple yet effective fractional order $PI^{\lambda}D^{\mu}A$ controller design method. The proposed design method uses only the step response of the stable process to be controlled and requires no process model.

The parameters of the fractional order PI$^{\lambda}$D$^{\mu}$A controller are tuned such that the closed loop system is equivalent to fractional Bode's ideal model a widely used fractional order model in the fractional order control domain because of its iso-damping property which is an important robustness feature. The main advantage of the proposed design method is that the useful tuning formulae of the fractional order PI$^{\lambda}$D$^{\mu}$A controller parameters are derived analytically without any complicated numerical calculations.

With the proposed methodology we get closed-loop systems robust to gain variations and step responses exhibiting an iso-damping property.

The benefit of the fractional order PI$^{\lambda}$D$^{\mu}$A controller design method is so simple and analytical that one can use the proposed tuning algorithm step-by-step.

Finally, the effectiveness of the proposed method is illustrated by numerical simulations and comparisons.

The further work is to investigate the discretization for fractional operator such that the proposed fractional order PI$^{\lambda}$D$^{\mu}$A controller can be applied in a real control system.

References

[1] D.J. Wang: Further results on the synthesis of PID controllers. *IEEE Transactions on Automatic Control*, **52**(6), (2007), 1127–1132. DOI: 10.1109/TAC.2007.899045.

[2] K.J. Astrom and T. Hagglund: *PID Controllers: theory, design and tuning*. Instrument Society of America, Research Triangle Park, North Carolina, U.S.A, 1995.

[3] J.G. Ziegler and N.B. Nichols: Optimum settings for automatic controllers. *Transactions of the ASME*, **64**(8), (1942), 759–768.

[4] R.C. Dorf and D.R. Miller: A method for enhanced PID controller design. *Journal of Robotics and Automation*, **6** (1991), 41–47.

[5] S. Jung and R.C. Dorf: Analytic PIDA controller design technique for a third order system. *Proceedings of the 35th IEEE Conference on Decision and Control*, (1996), 2513–2518. DOI: 10.1109/CDC.1996.573472.

[6] P. Ukakimaparn, P. Pannil, P. Boonchuay and T. Trisuwannawat: PIDA controller designed by Kitti's method. *ICCAS-SICE 2009 (ICROS-SICE International Joint Conference) Fukuoka, Japan*, (2009), 1547–1550.

[7] K. Smerpitak, P. Ukakimaparn, T.Trisuwannawat and P. La-Orsri: Discrete-time PIDA controller designed by Kitti's method with bilinear transform. *2th International Conference on Control, Automation and Systems (ICCAS)*, (2012), 1585–1590.

[8] S. Sornmuang and S. Sujitjorn: GA-based PIDA control design optimization with an application to AC motor speed control, *International Journal of Mathematics and Computers in Simulation*, **4**(3), (2010), 67–80.

[9] D. Puangdownreong: Application of current search to optimum PIDA controller design. *Intelligent Control and Automation*, **3** (2012), 303–312. DOI: 10.4236/ica.2012.34035.

[10] D.K. Sambariya and D. Paliwal: Optimal design of PIDA controller using firefly algorithm for AVR power system. *International Conference on Computing, Communication and Automation (ICCCA)*, (2016). DOI: 10.1109/CCAA.2016.7813859.

[11] D.K. Sambariya and D. Paliwal: Design of PIDA controller using bat algorithm for AVR power system. *Advances in Energy and Power*, **4**(1), (2016), 1–6. DOI: 10.13189/aep.2016.040101.

[12] C.U. Thaiwasin, S. Sujitjorn, Y. Prempraneerach and J. Ngamwiwit: Torsional resonance suppression via PIDA controller. *Proceedings of TENCON 2000*, (2000), 498–503. DOI: 10.1109/TENCON.2000.892316.

[13] S. Sunisa and S. Sarawut: GA-based PIDA control design optimization with an application to AC motor speed control. *International Journal of Mathematics and Computers in Simulation*, **4**(3), (2010).

[14] D.Y. Ha, I.Y. Lee, Y.S. Cho, Y.D. Lim and B.K. Choi: The design of PIDA controller with pre-compensator. *2001 IEEE International Symposium on Industrial Electronics Proceedings (Cat. No. 01TH8570)* (2001), 798–804.

[15] D.K. Sambariya and D. Paliwal: Comparative design and analysis of PIDA controller using Kitti's and Jung-Dorf approach for third order practical systems. *British Journal of Mathematics & Computer Science*, **16**(5), (2016), 1–16. DOI: 10.9734/BJMCS/2016/26223.

[16] K. Anand and A. MdNishat: A PID and PIDA controller design for an AVR system using frequency response matching. *International Journal of Innovative Technology and Exploring Engineering*, **8**(10), (2019), 1675–1681. DOI: 10.35940/ijitee.J8907.0881019.

[17] K. Mahendra and V.H. Yogesh: Robust IMC-PIDA controller design for load frequency control of a time delayed power system. *58th IEEE Conference on Decision and Control*, (2019). DOI: 10.1109/CDC40024.2019.9029259.

[18] K. Mahaendra and H. Yogeshv: Robust CDA-PIDA control scheme for load frequency control of interconnected power systems. *IFAC paper on line*, **51**(4), (2018), 616–621. DOI: 10.1016/j.ifacol.2018.06.164.

[19] T. Chaiyo, L. Kittisak, P. Deacha, S. Supaporn, H. Sarot and N. Auttarat: Application of bat-inspired algorithm to optimal PIDA controller design for liquid-level system. *International Electrical Engineering Congress IEECON 2018*, (2018). DOI: 10.1109/IEECON.2018.8712168.

[20] N. Auttarat, T. Chaiyo and P. Deacha: Application of spiritual search to optimal PIDA controller design for cardiac pacemaker. *4th International Conference on Digital Arts, Media*, (2019). DOI: 10.1109/ECTI-NCON.2019.8692275.

[21] P. Noppadol, P. Deacha, T. Chaiyo and H. Sarot: Obtaining optimal PIDA controller for temperature control of electric furnace system via flower pollination algorithm. WSEAS Transactions on Systems and Control, **14** (2019), 1–7.

[22] I. Podlubny: *Fractional Differential Equations*, Academic Press, San Diego, 1999.

[23] C.A. Monje, Y.Q. Chen, B.M. Vinagre, D. Xue and V. Feliu: *Fractional-order systems and controls: Fundamentals and Applications*. Sringer, 2010.

[24] K. Bettou and A. Charef: Control quality enhancement using fractional PI$^{\lambda}$D$^{\mu}$ controller. *International Journal of System Sciences*, **40**(8), (2009), 875–888. DOI: 10.1080/00207720902974546.

[25] D. Valério and J.S.D. Costa: Tuning of fractional PID controllers with Ziegler Nichols type rules. *Signal Processing*, **86**(10), (2006), 2771–2784. DOI: 10.1016/j.sigpro.2006.02.020.

[26] F. Padula and A. Visioli: Tuning rules for optimal PID and fractional order PID controllers. *Journal of Process Control*, **21**(1), (2011), 69–81. DOI: 10.1016/j.jprocont.2010.10.006.

[27] P.D. Mandić, T.B. Šekara, M.P. Lazarević and M. Bošković: Dominant pole placement with fractional order PID controllers: D–decomposition approach. *ISA Transactions*, (2017), 67–76. DOI: 10.1016/j.isatra.2016.11.013.

[28] B. Maâmar and M. Rachid: IMC-PID fractional order filter controllers design for integer order systems. *ISA Transactions*, **53**(5), (2014), 1620–1628. DOI: 10.1016/j.isatra.2014.05.007.

[29] M. Bettayeb and R. Mansouri: Fractional IMC–PID filter controllers design for non-integer order systems. *Journal of Process Control*, **24**(4), (2014), 261–271. DOI: 10.1016/j.jprocont.2014.01.014.

[30] R.S. Barbosa, J.A.T. Machado and I.M. Ferreira: Tuning of PID controllers based on Bode's ideal transfer function. *Nonlinear Dynamics*, **38** (2004), 305–321. DOI: 10.1007/s11071-004-3763-7.

[31] X. Li, Y. Wang, N. Li, M. Han, Y. Tang and F. Liu: Optimal fractional order PID controller design for automatic voltage regulator system based on reference model using particle swarm optimization. *International Journal of Machine Learning and Cybernetics*, **8**(5), (2017), 1595–1605. DOI: 10.1007/s13042-016-0530-2.

[32] M. Bettayeb, R. Mansouri and U. Al-Saggaf: Smith predictor based fractional order filter PID controllers design for long time delay systems. *Asian Journal of Control*, **19**(2), (2016), 587–598. DOI: 10.1002/asjc.1385.

[33] C.A. Monje, B.M. Vinagre, V. Feliu, and Y. Chen: Tuning and auto-tuning of fractional order controllers for industry applications. *Control Engineering Practice*, **16**(7), (2008), 798–812. DOI: 10.1016/j.conengprac.2007.08.006.

[34] H. Li, Y. Luo and Y. Chen: A fractional order proportional and derivative (FOPD) motion controller: Tuning rule and experiments. *IEEE Transactions on Control Systems Technology*, **18**(2), (2010), 516–520. DOI: 10.1109/TCST.2009.2019120.

[35] S.K. Verma and R. Devarapalli: Fractional order $PI^{\lambda}D^{\mu}$ controller with optimal parameters using modified grey Wolf optimizer for AVR system. *Archives of Control Sciences*, **32**(2), (2022), 429–450. DOI: 10.24425/ACS.2022.141719.

[36] M. Tenoutit, N. Maamri and J. Trigeassou: An output feedback approach to the design of robust fractional PI and PID controllers. *IFAC Proceedings Volumes*, **44**(1), (2011), 12568–12574. DOI: 10.3182/20110828-6-IT-1002.01217.

[37] A. Oustaloup: *La Commande CRONE: Commande robuste d'ordre non entier*. Hermès Science Publications, 1991 (in French).

[38] H. Wang, G.Q. Zeng, Y.X. Dai, D. Bi, J. Sun and X. Xie: Design of a fractional order frequency PID controller for an islanded microgrid: A multi-objective extremal optimization method. *Energies*, **10**(10), (2017), 1502. DOI: 10.3390/en10101502.

[39] G.Q. Zeng, J. Chen, Y.X. Dai, L. M. Li, C.W. Zheng and M.R. Chen: Design of fractional order PID controller for automatic regulator voltage system based on multi-objective extremal optimization. *Neurocomputing*, **160** (2015), 173–184. DOI: 10.1016/j.neucom.2015.02.051.

[40] I. Podlubny: Fractional-order systems and PI$^{\lambda}$D$^{\mu}$ controllers. *IEEE Transactions on Automatic Control*, **44**(1), (1999), 208–214. DOI: 10.1109/9.739144.

[41] K. Bettou and A. Charef: Optimal tuning of fractional order PI$^{\lambda}$D$^{\mu}$A controller using particle swarm optimization algorithm. *IFAC PapersOnLine*, **50**(1), (2017), 8084–8089. DOI: 10.1016/J.IFACOL.2017.08.1241.

[42] K. Bettou and A. Charef: Optimal fractional order PI$^{\lambda}$D$^{\mu}$A controller design for bioreactor control using particle swarm optimization. *6th International Conference on Systems and Control*, (2017). DOI: 10.1109/ICoSC.2017.7958652.

[43] K. Bettou and A. Charef: Tuning of fractional PI$^{\lambda}$D$^{\mu}$A controllers by using PSO. *International Journal of Control, Energies and Electrical Engineering (CEEE)*, **14** (2019), 30–34.

[44] C. Montree, N. Auttarat and P. Deacha: Optimal tuning of fractional order PI$^{\lambda}$D$^{\mu}$A$^{\nu}$ controller by cuckoo search algorithm. *2nd Artificial Intelligence and Cloud Computing Conference*, (2019), 178–183. DOI: 10.1145/3375959.3375960.

[45] P. Deacha: A novel fractional order PI$^{\lambda}$D$^{\mu}$A$^{\nu}$ controller and its design optimization based on spiritual search. International Review of Automatic Control, 12(6), (2019), DOI: 10.15866/ireaco.v12i6.17456.

[46] O. Necati, Y. Celaleddin, B.A. Baris, H. Norbert, K. Aslihan and S. Roman: 2DOF multi-objective optimal tuning of disturbance reject fractional order PIDA controllers according to improved consensus oriented random search method. *Journal of Advanced Research*, **25** (2020), 159–170. DOI: 10.1016/j.jare.2020.03.008.

[47] M. Ramasamy and S. Sundaramoorthy: PID controller tuning for desired closed-loop responses for SISO systems using impulse response. *Computers and Chemical Engineering*, **32** (2008), 1773–1788. DOI: 10.1016/j.compchemeng.2007.08.019.

[48] N. Fergani and A. Charef: Process step response based fractional $PI^{\lambda}D^{\mu}$ controller parameters tuning for desired closed loop response. *International Journal of Systems Science*, (2014), 512–532. DOI: 10.1080/00207721.2014.891667.

[49] A. Charef: Modeling and analog realization of the fundamental linear fractional order differential equation. *Nonlinear Dynamics*, **46** (2006), 195–210. DOI: 10.1007/S11071-006-9023-2.

[50] K. Miller and B. Ross: *An introduction to the fractional calculus and fractional differential equations*, Wiley, New York; 1993.

[51] I. Petras, I. Podlubny, P. O'Leary, L. Dorcak and B.M. Vinagre: Analogue realization of fractional order controllers. *Nonlinear Dynamics*, **29**(1–4), (2002), 281–296. DOI: 10.1023/A: 1016556604320.

[52] A. Charef, M. Charef, A. Djouambi and A. Voda: New perspectives of analog and digital simulations of fractional order systems. *Archives of Control Sciences*, **27**(1), (2017), 91–118. DOI: 10.1515/acsc-2017-0006.